Available online at www.sciencedirect.com
SCIENCE DIRECT
ELSEVIER
Continental Shelf Research 26 (2006) 385–400
CONTINENTAL SHELF RESEARCH
www.elsevier.com/locate/csr

The structure of tides in the Western Iberian region

Martinho Marta-Almeida*, Jesús Dubert

University of Aveiro, Department of Physics, 3810-193 Aveiro, Portugal

Received 22 October 2004; received in revised form 10 October 2005; accepted 30 November 2005
Available online 13 February 2006

Abstract

A s-coordinate three-dimensional model, regional ocean modeling system (ROMS), was implemented in the Western Iberian region ranging from the coast to 11°W aiming high-resolution tidal simulations for an homogeneous ocean. The features for tidal heights and ellipses for the principal constituents, M_2, S_2, N_2, K_2, K_1, O_1, P_1 and Q_1, were imposed at the boundaries of the model. A tidal analysis for heights and tidal currents was done allowing to calculate two-dimensional distribution of amplitudes and three-dimensional structure of tidal currents. The amplitudes and phases for heights agree with previous results and observations, showing a good precision on the tidal propagation in the interior of the domain. Tidal kinetic energy is dominated by the semi-diurnal components, mainly M_2, and increases on the shelf. Over the Lisbon Promontory the diurnal component K_1 is however the second more energetic harmonic. Vertical variation of tidal ellipse parameters evidences the different structure of semi-diurnal and diurnal tidal components, as well as differences between the open sea and shelf tidal circulation.

Keywords: Tidal heights and currents; Tidal ellipses; Western Iberian tides; Three-dimensional tidal circulation

1. Introduction

The main aim of this work is to study the tides and its associated currents in the shelf/slope of western Iberian Peninsula based on a three-dimensional (3-D) model. In spite of a large number of studies and observational programmes on this region were (and are) devoted to subinertial aspects of the circulation at the shelf/slope, much less studies about the tidal dynamics in this region can be found.

The Western Iberian Peninsula (Fig. 1) extends approximately south–north along the meridian 9°W, between 37°N and 43°N. The shelf width is approximately 40 km unless in the southernmost region, until Lisbon, where it is half of this value. The region is characterised by the presence of several irregularities determinant for the tidal dynamics, namely the Lisbon Promontory (LP) and four main canyons: Setúbal, Nazaré, Aveiro and Porto. The bathymetry profile from cape S. Vicente to Setúbal Canyon is characterised by the lack of a clear shelf break and the depth increases in a near exponential manner.

Previous work has already been done in this region using also a 3-D model (Fanjul et al., 1997) and using bidimensional finite elements models (Sauvaget et al., 2000; Fortunato et al., 2002). Fanjul et al. (1997) performs a very extensive analysis of the tidal propagation for the eastern North Atlantic region. They put a special emphasis

*Corresponding author. Tel.: +351 9147 17533.
E-mail address: martinho@fis.ua.pt (M. Marta-Almeida).

0278-4343/$ - see front matter © 2006 Elsevier Ltd. All rights reserved.
doi:10.1016/j.csr.2005.11.011

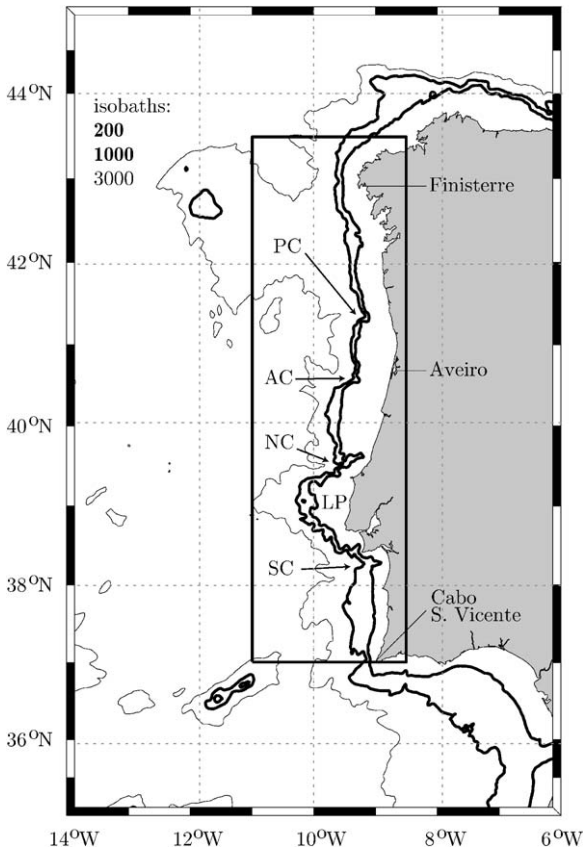

Fig. 1. Region of study with modelling area (inner rectangle). Slope is given by isobaths 200 m and 1000 m (bold isobaths). Isobath 3000 is also included. The main bathymetric irregularities are shown, namely the Setúbal Canyon (SC), the Lisbon Promontory (LP), the Nazaré Canyon (NC), the Aveiro Canyon (AC) and the Porto Canyon (PC). The dimensions of the modelling area are 720 km in the south–north direction and 210 km in the west–east direction.

in comparison with observational data (tidal gauges and currentmeters on the French shelf) and achieve a very accurate description in terms of the propagation of the tidal wave. However, their model configuration is not designed to study the details of the adjustment of the tidal wave in the shelf/slope region. Bidimensional modelling study of Sauvaget et al. (2000) is centred mainly on the numerical formulation of the finite elements model and the comparison of amplitudes and phases with tidal gauges registers. Fortunato et al. (2002) also with finite element modelling approach, give emphasis to the generation of barotropic shelf waves arising from diurnal tides at the LP. The main feature of the above-cited works is an accurate comparison of amplitudes and phases of the main tidal constituents with observational data (tidal gauges). The main emphasis of this work will be to carry out a study of some 3-D aspects of the adjustment of the tidal ellipses at the shelf/slope, namely, the horizontal structure (amplitude and polarisation) and the vertical structure in the water column. However, some comparisons of tidal heights and tidal currents are done to assure the model results validation.

For several years, two-dimensional models gave adequate results for predictions of tidal elevations. However, because of much small scale variability of tidal currents, in comparison with elevations, a rigorous study of tidal dynamics on the shelf requires an high resolution 3-D numerical model (Prandle, 1997b; Davies et al., 1997). This is a consequence of the higher bottom and internal frictional influence in these regions (Prandle, 1997a). Because diurnal currents are more sensitive to friction than the semi-diurnals currents of the same magnitude (Prandle, 1997b), this may be a justification to the fact that in the above mentioned previous studies, diurnal constituents exhibit larger deviations when compared with available data.

Many results of this work are built upon previous theoretical and observational works on tidal dynamics. A good explanation of the vertical tidal ellipse variation was given by Prandle (1982) for the homogeneous case and some other studies for the stratified ocean also exist (Souza and Simpson, 1996; Simpson, 1997; Xing and Davies, 1997, 1998).

The stratification is not considered in this study, neglecting the internal tide associated with the interaction between steep topography, the startification and the barotropic tide. Although we do not expect that the influence of internal wave propagation to be so large as in Bay of Biscay (New and da Silva, 2002) or in Malin-Hebrides region (Xing and Davies, 1998), some evidences from internal tide tidal currents can be found in Vitorino et al. (2002), which reports bottom intensification and cross-shore polarisation of currents along the Porto Canyon axis, over the shelf. However, the comparison of tidal ellipses of stations located in the inner shelf reported in this work indicates that the effects of stratification in tidal currents are not important in that region. Also, it is not expected that the amplitude and phase of tidal wave be significantly affected by stratification, similarly to the Xing and Davies (1998) study.

The following section describes the model setup and parameterisation. Section 3 includes the results

and its analysis being divided in analysis of tidal heights, analysis of tidal currents, analysis of the vertical structure of tidal ellipse parameters and analysis of sensitivity of the results to the bottom friction. In Section 4 the results are summarised.

2. Model setup and parameterisation

A 3-D model was used to simulate tidal dynamics in the Western Iberian Peninsula Coast. The model is ROMS (Haidvogel et al., 2000), a free surface, hydrostatic, primitive equations model, with vertical s-coordinates (Song and Haidvogel, 1994).

The grid used covers the longitudes between 8.5°W and 11°W and the latitudes 37°N–43.5°N (Fig. 1), thus 720 km in the south–north direction and 210 km in the west–east direction. Grid resolution is constant with ~0.75 km in the zonal (W–E) direction and ~2 km in the meridional (S–N) direction, consisting in 280 by 360 grid points. Ten vertical s-levels were used, with $\theta_s = 3$ and $\theta_b = 0.4$, as defined by Song and Haidvogel (1994), indicating that vertical resolution is increased in surface and bottom.

In this study, homogeneous conditions for temperature and salinity, with values $T = 14\,^{\circ}\mathrm{C}$ and $S = 35$ psu, were used.

Grid topography was taken from General Bathymetric Chart of the Oceans (GEBCO) 1-min global bathymetric grid, with some corrections on the continental shelf.

ROMS was forced at the open boundaries with tidal parameters for elevations (amplitudes and phases) and for current ellipses (semi-major axis, semi-minor axis, inclination and phase). Tidal data was obtained from OSU TOPEX/Poseidon Global Inverse Solution, TPXO (Egbert and Erofeeva, 2002). TPXO is a global model of ocean tides, which best suits the Laplace tidal equation and data from the TOPEX/Poseidon orbit cycles. It uses a inversion scheme (Egbert et al., 1994) developed for assimilating the altimetric data into a global barotropic model. That model provides elevations and tidal currents for the main semi-diurnal and diurnal constituents (M_2, S_2, N_2, K_2 and K_1, O_1, P_1, Q_1, respectively) with a resolution of 1/6° for the North Atlantic. As a first approach, barotropic initial conditions were used. The model was ran for 60 days and the output time series of ocean surface heights and ocean currents was analysed, using harmonic least squares fit, to retrieve harmonic parameters of tides. The output time series were separated by 5 grid points, in both S–N and W–E direction, i.e., with a resolution of 10 per 3.75 km, respectively.

The simulation period was smaller than synodic period of some pairs of constituents, following Rayleigh criterion. In the case of S_2 and K_2, or K_1 and P_1, the time series length should be at least 182 days. However, using Fourier analysis it was realised that shallow water tidal constituents are not important in the studied region. For this reason, the least-squares fit was done only with the forcing frequencies becoming the Rayleigh criterion unnecessary.

Model setup parameters are shown in Table 1. The vertical mixing scheme is based on the vertical closure turbulent model proposed by Large et al. (1994) (*K*-profile parameterisation, KPP).

Due to the importance of the bottom friction for the tidal currents on the shelf, four simulations were performed in order to test the sensitivity of the parameterisation of the bottom friction on the tidal dynamics (Table 2). In three simulations, a linear bottom friction condition ($\tau_b = rv_b$, where v_b stands for the velocity at the deepest level), with different bottom drag coefficients, r, was used. In one simulation a typical value of $r = 3 \times 10^{-4}$ m s^{-1} was used, and in the other two, half and the double of this value. In the fourth simulation, a quadratic formulation, $\tau_b = C_d v_b U_b$, where v_b is an horizontal current component at the deepest level, U_b is the horizontal speed at the same level and $C_d = (k/\ln(z_b/z_0))^2$, with $k = 0.4$ von Kármáan's

Table 1
Model setup parameters

L	280	No. points E–W
M	360	No. points N–S
N	10	No. of *s*-levels
$h_{\max}$	5125 m	Maximum region depth
$h_{\min}$	5 m	Minimum region depth
θ_s	3	*S*-coordinates surface control parameter
θ_b	0.4	S-coordinates bottom control parameter
Δx	0.75 km	Resolution in the zonal direction
Δy	2 km	Resolution in the meridional direction
Δt	60 s	Baroclinic time step
Δt_f	3 s	Barotropic time step
ν	15 m^2 s^{-1}	Laplacian horizontal viscosity
ν_t	15 m^2 s^{-1}	Laplacian horizontal diffusivity
κ	5×10^{-6} m^2 s^{-1}	Background vertical viscosity
κ_t	5×10^{-6} m^2 s^{-1}	Background vertical diffusivity
r	3×10^{-4} m s^{-1}	Linear bottom drag coefficient (run II)
T	14 °C	Constant temperature
S	35 psu	Constant salinity

Table 2
Simulations performed to test the sensitivity of the bottom friction parameterization on the tidal dynamics

Run	Bottom frict. parametriz.	Friction parameter
I	Linear	$r = 1.5 \times 10^{-4}\,\mathrm{m\,s^{-1}}$
II	Linear	$r = 3.0 \times 10^{-4}\,\mathrm{m\,s^{-1}}$
III	Linear	$r = 6.0 \times 10^{-4}\,\mathrm{m\,s^{-1}}$
IV	Quadratic	$z_0 = 0.005\,\mathrm{m}$

The parameter r is the linear bottom drag coefficient and z_0 is the bottom roughness of the quadratic formulation.

constant, z_b the height of the deepest level and z_0 the bottom roughness was used. For z_0, a typical value of 0.005 m was used.

3. Results

The characteristics of the slope and the latitudinal variations in bathymetry lead to important modifications in the offshore tidal wave, originally moving northwards as a Kelvin wave. Acting as a barrier to the tidal wave propagation, the relatively wide LP (see Fig. 1) is an important topographic feature in the studied region. In this area, different relative amplification of tidal constituents originates an interesting horizontal tidal currents pattern, with currents in opposite directions at points separated by few dozens of kilometres at the shelf, analysed below.

Tides in the Western Iberian Coast are dominated by the semi-diurnal tidal components M_2 and S_2 (Figs. 2 and 3), which give rise to clear spring-neap cycles modulated by other constituents. In some parts of the shelf like LP, however, diurnal harmonics, especially K_1, assume a great importance and modifies significantly the tidal currents pattern.

The results presented hereinafter, namely the tidal heights, tidal currents and vertical structure are the results of the main simulation (Table 2, run II), with linear drag coefficient $r = 3 \times 10^{-4}\,\mathrm{m\,s^{-1}}$. At the end of this section, the sensitivity to bottom friction is analysed by comparing the results of the main simulation with the other simulations, with different bottom friction parameterisations (Table 2).

3.1. Tidal heights

Figs. 2 and 3 show cotidal charts for the semi-diurnal and diurnal tidal components. Results are in agreement with Fanjul et al. (1997). Tidal wave propagates from south to north as a Kelvin wave with amplitudes decreasing offshore. Highest tidal amplitudes are found in the north of the region. M_2 is the main harmonic with amplitudes around 1 m, followed by S_2 with less than half of this value, N_2 with 0.25 m and K_2 with 0.1 m. Diurnal components show relative small values, around 0.08 m for K_1, 0.06 m for O_1, 0.02 m for P_1 and less than 0.02 m for Q_1. Exponential increase of amplitude towards the coast is found in all semi-diurnal charts for the generality of the region, and phase lines are perpendicular to the coast, while diurnal components do not show such behaviour. These components exhibit an amplification over LP and over the Galician shelf.

Table 3 shows a comparison of the simulated amplitudes and phases of tidal heights with analysis of observations done in Tables 3 and 4 of Fanjul et al. (1997), for two locations of the west coast of the Iberian Peninsula: Vigo and Cascais ports. We consider this comparison satisfactory, with amplitude differences of O(1 cm) and typical phase errors of 3° for semidiurnal components and 6° for diurnal ones, and provides confidence for the results analysed in this work.

3.2. Tidal currents

Figs. 4 and 5 show the tidal ellipses for the semi-diurnal and diurnal components calculated from the vertically integrated currents. The blue ellipses are conterclockwise and the red ones are clockwise.

Pure Kelvin wave dynamics expects current ellipses rotating counterclockwise and aligned parallel to the coast. By these figures we realise that if this happens approximately in the open sea, it is not the case of the shelf region. Bathymetric irregularities have large influence in the adjustment of the velocity field. It is responsible for amplification of tidal currents, inversion of the direction of rotation of the tidal ellipses and its polarisation in certain directions.

The S–N orientation of tidal currents changes in presence of the shelf features. In southern region, where slope is smooth this influence is not relevant. On the other hand, because of the steep slope of northern region, semidiurnal components suffer amplification and ellipses become polarised orthogonally to bathymetric lines. This behaviour has been observed in other places, recently by de Mesquita (2003) and Pereira et al. (2002), for

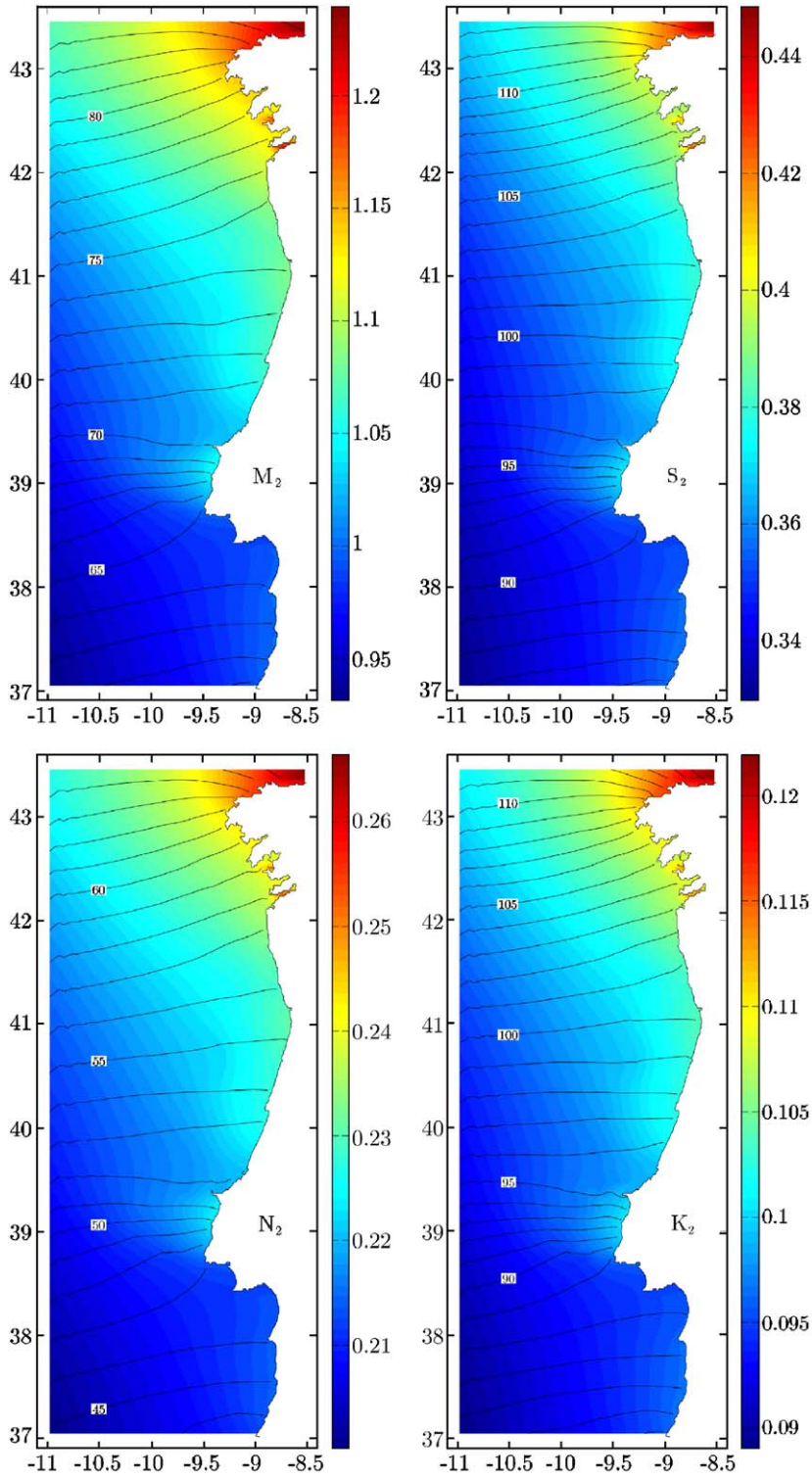

Fig. 2. Amplitudes (m) and Greenwich phases (deg) isolines of the semi-diurnal tidal components: M_2, S_2, N_2 and K_2.

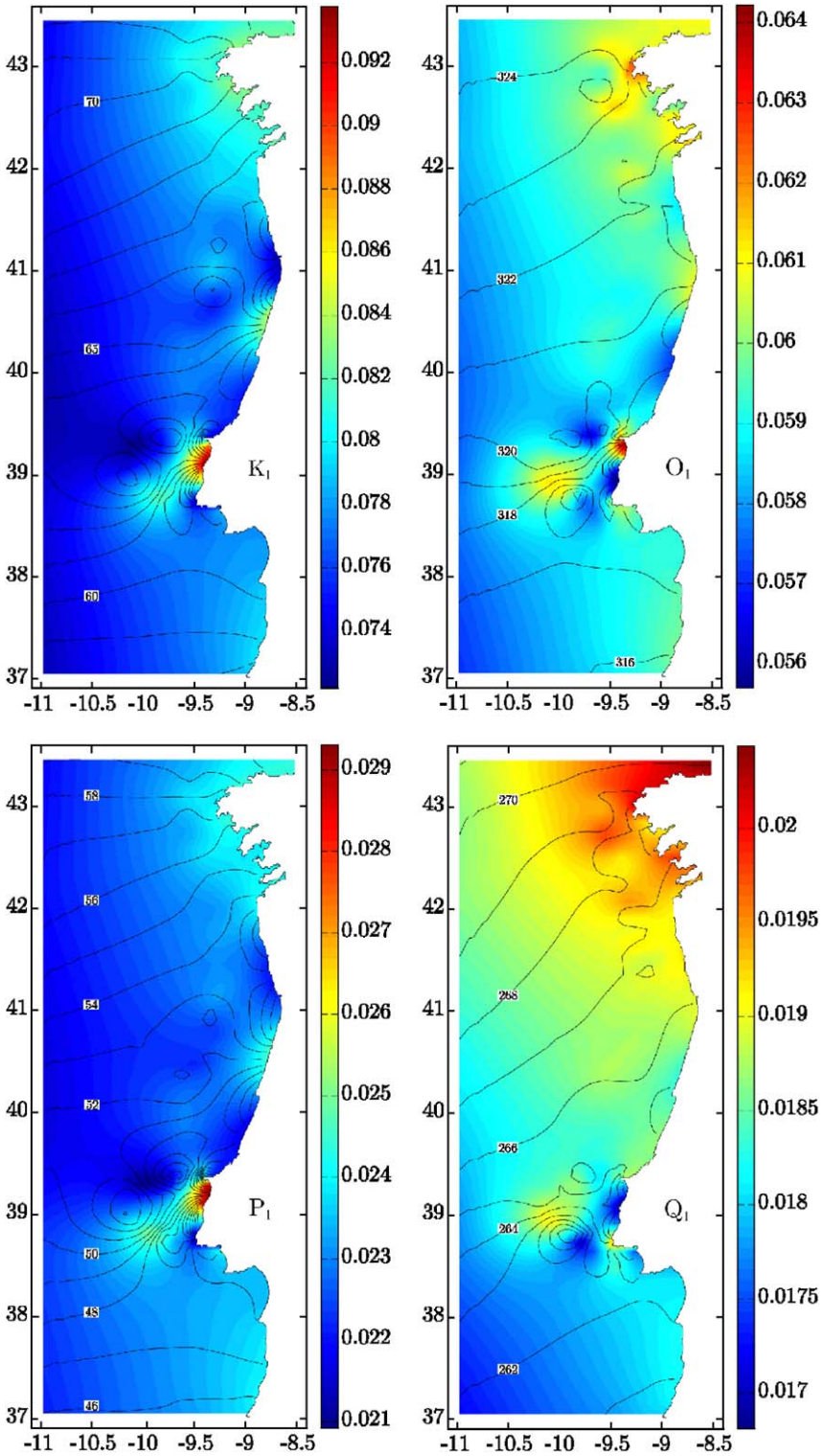

Fig. 3. Amplitudes (m) and Greenwich phases (deg) isolines of the diurnal tidal components: K_1, O_1, P_1 and Q_1.

Table 3
Simulated and observed amplitudes and phases of tidal heights for Cascais and Vigo

	Cascais				Vigo			
	Amplitude (cm)		Phase (deg)		Amplitude (cm)		Phase (deg)	
	Obs	Sim	Obs	Sim	Obs	Sim	Obs	Sim
M_2	112.3	113.2	65.0	64.8	112.3	113.2	76.7	80.0
S_2	35.0	35.3	91.0	90.3	38.8	39.7	106.2	109.9
N_2		21.3		47.0	23.8	23.9	58.1	61.1
K_2		9.5		88.6	11.0	10.8	103.8	106.7
K_1	7.0	7.7	54.0	60.1	7.6	8.1	59.4	67.6
O_1	5.8	5.9	313.0	317.6	6.5	6.1	318.7	323.1
P_1		2.3		47.7	2.5	2.4	48.4	55.7
Q_1		1.8		262.7		1.9		267.8

Observed data is taken from Tables 3 and 4 of Fanjul et al. (1997).
Empty field is employed where no data is available.

Table 4
Relative percentage of kinetic energy density of depth averaged velocities

	Shelf/region	LP/region	Shelf/total	LP/total
All	62.02	30.71	62.02	30.71
SD	51.92	15.87	40.48	12.38
D	97.79	83.28	21.53	18.34
M_2	51.78	15.71	33.41	10.14
S_2	51.91	16.92	5.13	1.67
N_2	54.28	15.31	1.52	0.43
K_2	54.28	17.78	0.42	0.14
K_1	97.69	82.23	15.25	12.84
O_1	97.95	83.84	3.82t	3.27
P_1	98.40	89.53	2.14	1.94
Q_1	96.38	84.81	0.33	0.29

First column: rate between energy on shelf/upper slope of each component and energy of whole domain region for that component. Second column: rate between energy on Lisbon Promontory (LP) of each component and energy of whole domain region for that component. Third column: rate between energy on shelf/upper slope of each component and total energy of whole domain. Fourth column: rate between energy on LP of each component and total energy of whole domain.

instance, and it happens in places were the wave front crosses the slope. Associated with the depth increase or decrease, the change of wave speed leads to wave refraction which make the wave front to become oriented parallel with isobaths (Pugh, 1987). This phenomenon is clearer in places with larger slope, that is, between LP and Galicia and is not a feature of diurnal tides.

Of special interest when referring to diurnal tides in the studied area, is the LP. This is the place where larger ellipse amplification of diurnal components occurs, associated with the intensified tidal amplitudes in this region (Fig. 3).

Diurnal currents amplification in the Western Iberian shelf has been studied in terms of topographic waves (Sauvaget et al., 2000). In what concerns tidal currents structure, four regimes are noticeable: open sea/shelf and semi-diurnal/diurnal currents. Shelf tidal circulation completely differs from open sea dynamics for all tidal components; all semi-diurnal current ellipses exhibits similar behaviour with different scales and the same statement is valid for diurnal current ellipses.

To quantify the relative importance of tidal components currents and the differences between open sea and shelf regimes, the kinetic energy density averaged over the tidal period was calculated for each tidal component. This calculus was done as

$$\frac{1}{T_i}\int_0^{T_i}\frac{1}{2}\rho(U_i^2+V_i^2)\,\mathrm{d}t,$$

where T_i is the period of the tidal component i,

$$U_i = U_{0i}\cos\left(\frac{2\pi}{T_i}t+\phi_{ui}\right)$$

and

$$V_i = V_{0i}\cos\left(\frac{2\pi}{T_i}t+\phi_{vi}\right).$$

This integral results in $\rho(U_{0i}^2+V_{0i}^2)$. Considering the absence of spatial density differences, because we are interested in relative values (rates), the expression used for the kinetic energy density was $U_{0i}^2+V_{0i}^2$. Notice that the integral is independent of the number of periods used, i.e., the result is the same if we use nT, instead of T, for integer $n>1$.

Table 4 shows these values for the barotropic velocities. The first column represents the rate between energy on shelf/upper slope (inshore of isobath 1000 m) of each component and energy of whole domain for that component. The second one provides the rate between energy on LP of each component and energy of whole domain for that component. LP is here defined and the section of shelf between latitudes 38.5°N and 39.5°N. The third column represents the rate between energy on shelf/upper slope of each component and the total

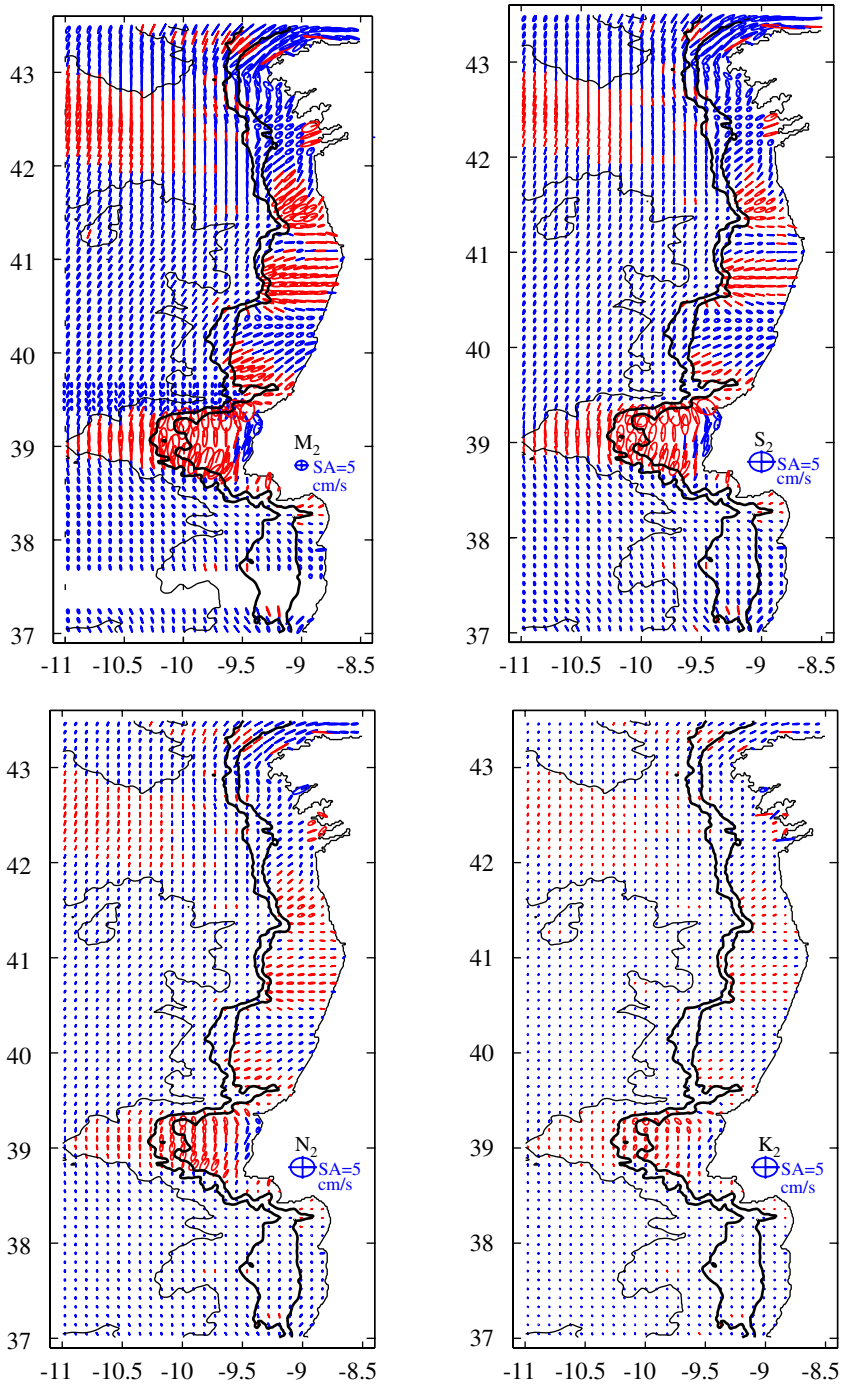

Fig. 4. Barotropic tidal ellipses of the semi-diurnal tidal components: M_2, S_2, N_2 and K_2. Blue ellipses are counterclockwise, while red ones have clockwise rotation. The radial line inside the ellipses gives the Greenwich phase. Over the Lisbon Promontory M_2 and S_2 ellipses are more disperse for clarity. Notice the ellipses scale. It represents a circular ellipse with semi-axis of $5\,cm\,s^{-1}$, but its size is half for M_2. Bold bathymetric lines represent the shelf break (200 and 1000 m); the thick line is the isobathymetric 3000 m.

energy (all components) of whole domain. The fourth column is the rate between energy on LP of each component and total energy of whole domain.

The distribution of energy from each component (columns 1 and 2) shows that between 96 and 98% of the diurnal energy is on the shelf, mainly over LP

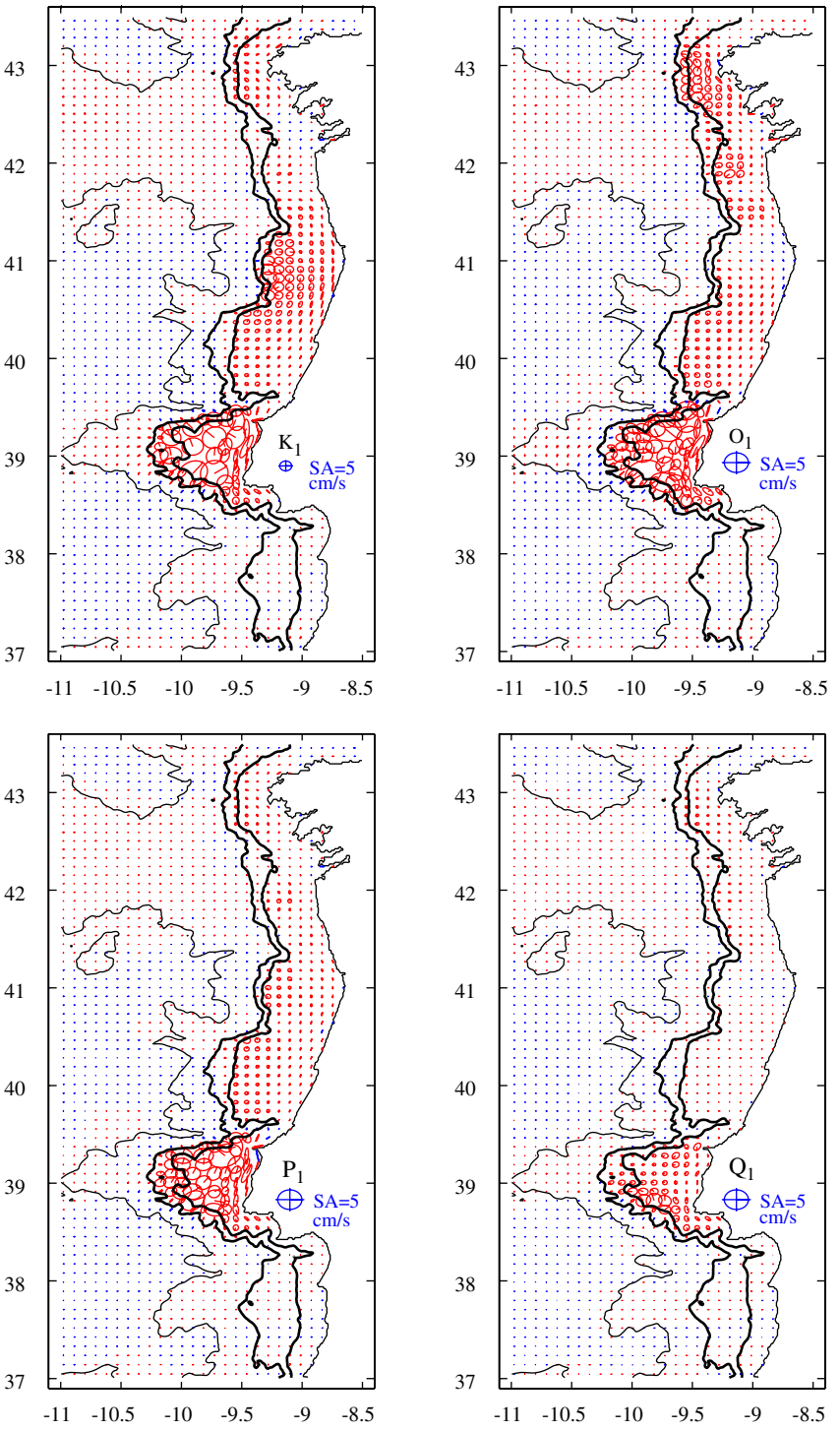

Fig. 5. Barotropic tidal ellipses of the diurnal tidal components: K_1, O_1, P_1 and Q_1. Blue ellipses are counterclockwise, while red ones have clockwise rotation. The radial line inside the ellipses gives the Greenwich phase. Notice that K_1 ellipse scale is the double or the others.

(second column, 82–90%). For the semi-diurnal components these values decrease to about 50% over the shelf and 15–18% over LP. Comparing the energy of each component with the total energy (columns 3 and 4) we see that M_2 represents 33.41% of the energy distribution and one third of it is

found over LP (10.14%). In the case of K_1 this proportion increases to almost one, 15.25% for the shelf and 12.84% for LP, indicating a concentration of diurnal energy on LP. The diurnal components dominate over LP (last column), where K_1 is the strongest component followed by M_2, O_1 and P_1.

Similar analysis has been done for surface and bottom velocities (not shown). For the surface, the shelf energy density shows higher values, mainly for the semi-diurnal components where the rate between the shelf and the full region for each component is now about 67% (it was about 52% in the case of barotropic velocities). Diurnal components remain closer to the barotropic value, about 99%. Over LP (second column), the diurnals have approximately the same value but the semi-diurnals, however, decrease to about one third of the barotropic case. The bottom velocities follow very close (qualitatively and quantitatively) what happens at the surface.

An example of the complex behaviour of the tidal currents is reported in Fig. 6 in which the tidal elevation during 10 days is represented in the upper side of the figure for two stations, located at the positions P1 and P2, of Fig. 7. Both graphics of tidal elevations are almost coincident because both stations are close. However the tidal currents present rather different patterns. Even if the stations are separated by ~50 km in the shelf of LP, the time evolution of the tidal current is almost opposite in intensity and direction, in such a way that during flooding flow tide the currents in the offshore station P1 are in the northward direction and rotating clockwise whereas in the coastal station P2 the flow has southward direction and it turns mainly in the counterclockwise direction, opposing to the surrounding flow. This occurs because at P1 diurnal currents are similar in amplitude to semi-diurnal currents, generating a pattern essentially diurnal, while in location P2, diurnal currents are much smaller than at P1 and the typical semi-diurnal modulation is observed.

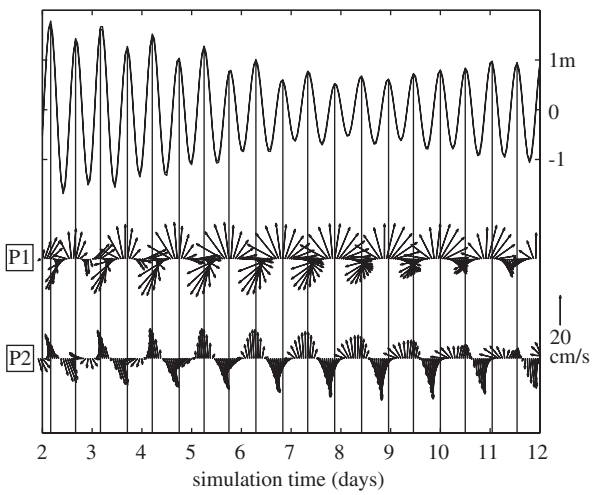

Fig. 6. Tidal heights and currents at the points P1 and P2 (see Fig. 7). Heights are superposed and are almost coincident. The vertical lines indicate the high tides.

The validation of tidal heights is basically based on previous studies for this region as was done in Table 3, indicating a good agreement between observation and modelling. For currents validation there are some available data from currentmeters. Fig. 8 is a comparison between M_2 ellipses obtained through analysis of data collected during the Survival cruise, described in Santos et al. (2004), during 2 weeks of February 2000. The harmonic analysis of these time series was done with the T_TIDE package (Pawlowicz et al., 2002). The currentmeters location is shown in Fig. 7 as C1 and C2. C1 was placed at 10 m depth, being the total depth 30 m. At C2 there were two currentmeters at depths 20 and 45 m, being the total depth 80 m. Taking into account the small length of the data series and the current variance, this comparison is considered quite good, giving confidence to the results obtained in this work.

3.3. Vertical structure

The vertical structure of tidal ellipses parameters—semi-major axis, eccentricity, inclination and phase angle—will now be discussed. Three region slices were chosen for this analysis according to its tidal circulation behaviour. In each slice were selected a variable number of sites either on open sea and shelf, where twenty equally spaced in depths harmonic analysis of currents (obtained through interpolation between the s-levels) was performed.

Slices locations are shown in Fig. 7a by I, II and III. Fig. 7b–d shows the grid vertical slices at these locations, together with position of the analysed sites—numbered vertical lines. S-coordinate levels are also shown. This figure is particularly useful to see the topographic differences of the slices. We remark the nonexistence of shelf break in the slice III, corresponding to southern region, in contrast

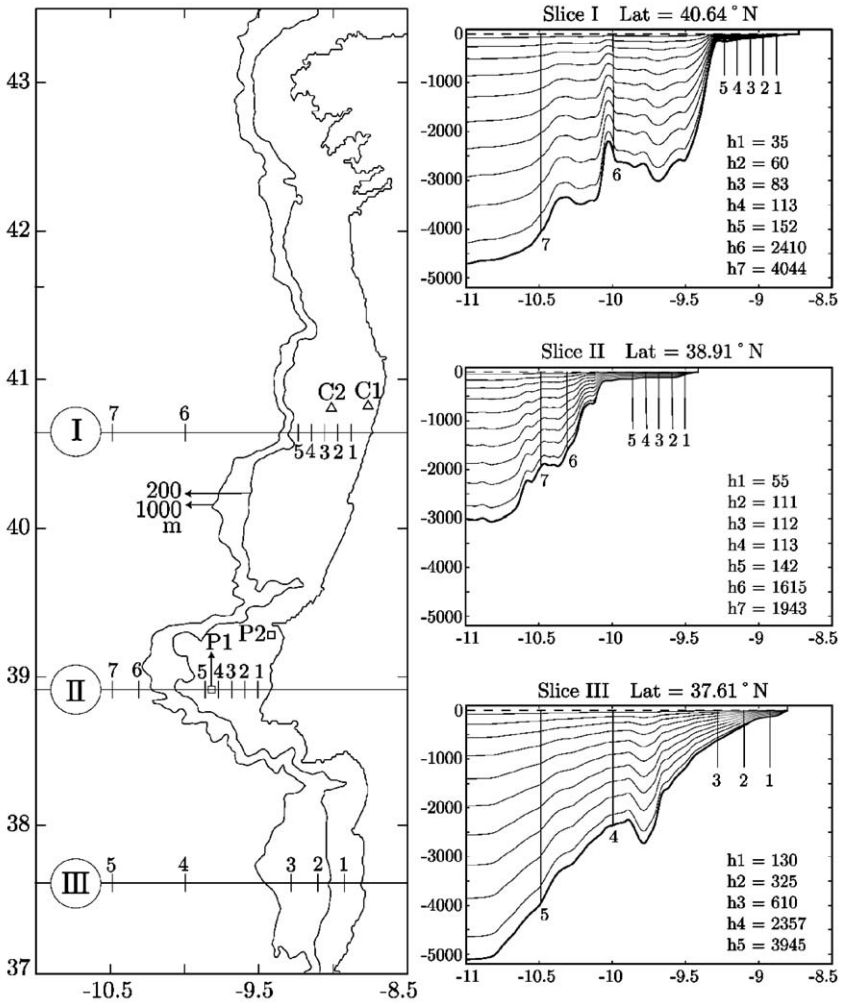

Fig. 7. Studied area (left) with locations referenced through the text, namely the slices I–III in which vertical variation of ellipses parameters was analysed (Figs. 9, 10 and 11); the currentmeters locations C1 and C2 (Fig. 8); the sites P1 and P2, for current inversion feature over Lisbon Promontory (Fig. 6). At right are shown the vertical slices I–III. The deepest line, bold, is the bathymetry. Other solid lines correspond to the s-coordinates levels. The numbered vertical lines are the sites where vertical analysis is done. The correspondent depths are also shown.

with the steep slope in the other slices—LP (II) and northern region (I).

In Figs. 9 and 10 are represented the vertical profile of ellipse parameters for M_2 and K_1, respectively. Numbered (bold) lines correspond to the sites at the shelf and numbers increase in the offshore direction. Open sea sites were not numbered because the lines in these figures are very close, indistinguishable in some cases. Only M_2 harmonic, as semi-diurnal, and K_1 harmonic, as diurnal, are shown, because other semi-diurnal and diurnal components follow qualitatively the same analyses. Notice that in these figures, the mean value of the ellipse parameters was removed. In the vertical, relative depth is used, being 0 the surface and −1 the bottom.

These figures evidence the distinction between open sea and shelf. Offshore vertical structure of the velocity field is independent of the depth. Indeed, for the offshore stations, vertical variations in ellipses parameters occur usually only near the bottom. On the other hand, in the shelf, the vertical modification of ellipses occurs in the entire water column, also associated with spacial variations from

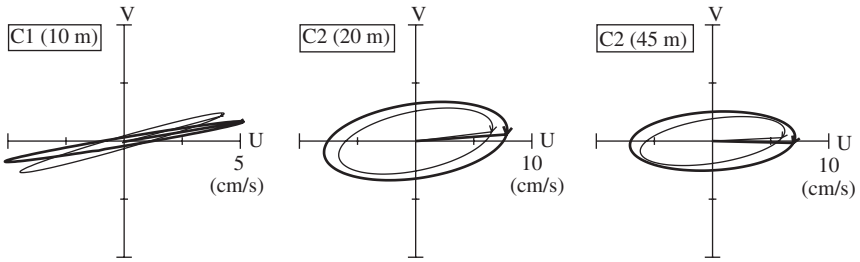

Fig. 8. Comparison of model results with currentmeters (bold line) for M_2. Currentmeters data was collected in February 2000 during the Survival campaign for 15 days at the sites C1 and C2 (see Fig. 7). These two points are located at 30 m and 80 m isobaths.

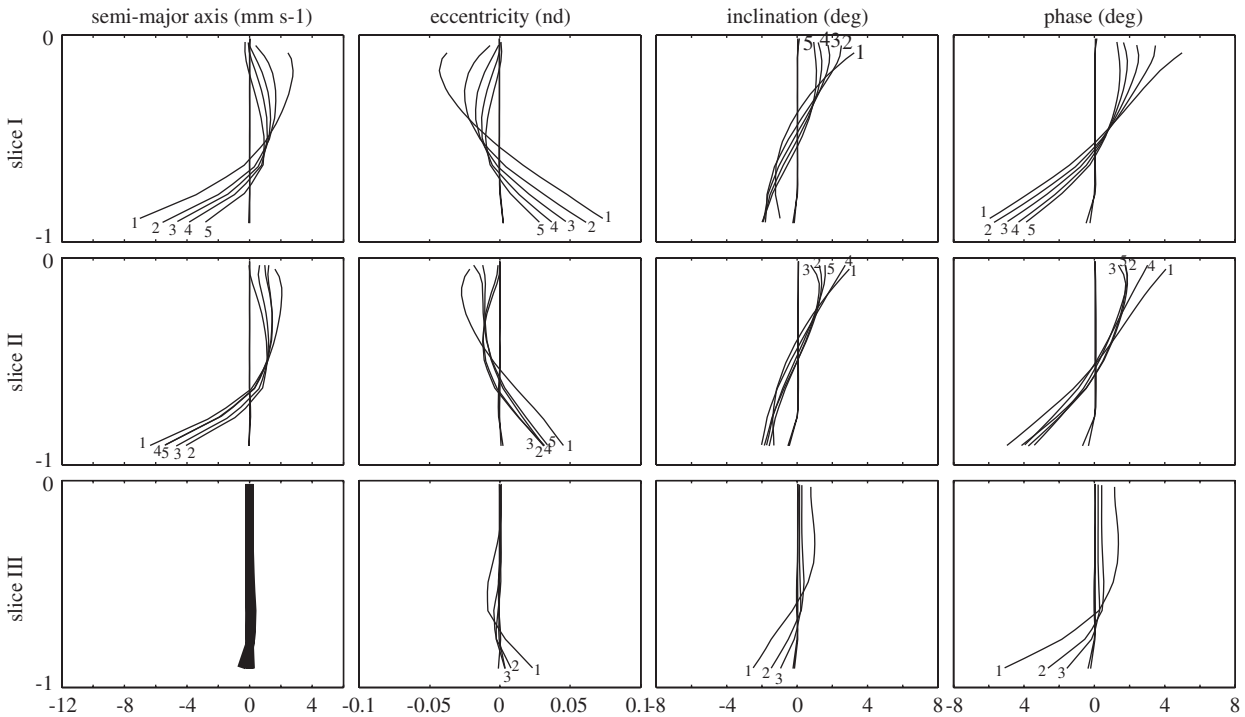

Fig. 9. Vertical structure of M_2 tidal ellipse parameters. Slice I is in front of Aveiro—first row; slice II crosses the Lisbon Promontory—second row; slice III is in the middle of the southern part of the modelled region—third row. See Fig. 7 for the location and properties of the slices. Variation with depth of ellipse parameters is represented: semi-major axis—first column; eccentricity—second column; ellipse inclination—third column; phase, relative to Greenwich—fourth column. Relative depth is used being 0 the surface and −1 the bottom. The mean of all ellipse parameters was removed for clarity. Units are $m\,s^{-1}$ for semi-major axis, degrees for inclination and phase. Eccentricity has no units.

slice to slice. Differences in the way diurnal and semi-diurnal tidal components change, not only spatially but vertically, are also shown.

Tidal components have larger semi-major axis (Figs. 9 and 10, first column) usually below the surface decreasing with depth. A typical variation of $O(1)\,cm\,s^{-1}$ in semi-major axis is found in all slices, for both M_2 and K_1, on the shelf except in slice III, located in the southern region, where the slope is very smooth (see Fig. 7). The largest surface to bottom variation occurs for the diurnal harmonic at the slices II, over the LP, where highest tidal current amplification exists. The vertical variation of ellipse amplitude and other parameters generally decrease offshore, until the shelf break, becoming the tidal structure essentially barotropic in the open sea.

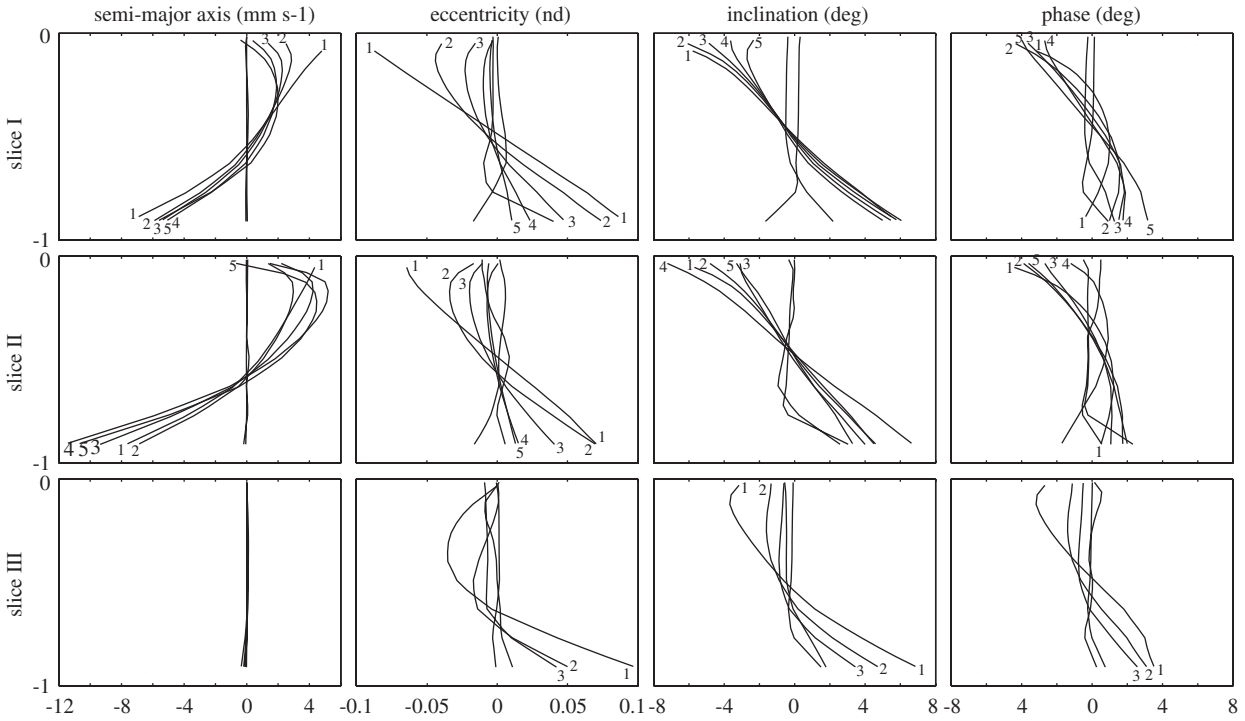

Fig. 10. Same as Fig. 9, but for the diurnal harmonic K_1.

Ellipse eccentricity (rate between semi-major and semi-minor axis; if 0 the ellipse is degenerated, a line segment; if 1 the ellipse is a counterclockwise circumference; if -1, the ellipse is a clockwise circumference) behaves in opposite way to semi-major axis. Highest eccentricity is found at the bottom indicating that ellipses become more counterclockwise with depth (positive eccentricity means counterclockwise ellipse rotation). Once again, variation with depth has a minimum below the surface (in the case of semi-major axis it was a maximum). Larger amplitude of vertical variation also increases onshore. K_1 eccentricity at offshore sites seems to be less barotropic than for M_2.

Ellipse inclination (angle between semi-major axis, in the first or second quadrant, and *u*-axis) also evidences difference between semi-diurnal and diurnal components. Semi-diurnal ellipses inclination shows smaller difference between open sea and shelf than diurnal ones. Also should be noticed that diurnal inclinations in open sea are more depth dependent than semi-diurnal, increasing in the last third of water depth, near the bottom. If slice III is almost barotropic respecting semi-major axis, it is not in terms of inclination, which shows a variation comparable to the other slices. Inclination vertical profile of diurnal components is opposite to the semi-diurnal one.

Tidal ellipses phase (the angle, relative to Greenwich meridian, the ellipse need for currents reach the maximum in the first or second quadrant) evidences similar behaviour. Semi-diurnal components have bigger vertical variation in the shelf than diurnal components phases. A typical variation of $O(10)^\circ$ almost linear between bottom and surface is found in the slice I and II for the semi-diurnal component. The variation in the diurnal K_1 component is about two thirds of the semi-diurnal M_2 phase's vertical variation. In the slice III the phases are almost constant in the first half of the water column (from surface to bottom).

3.4. Sensitivity to bottom friction

The vertical structure of tidal currents, mainly in shelf regions, is sensitive to bottom friction, which should be responsible for many of the features described until here. Fig. 11 shows the vertical variation of the tidal ellipses parameters at the shelf station I.4, shown in Fig. 7a. Each row corresponds to one of the four runs done to test the sensitivity of the model to bottom friction (Table 2). The bold

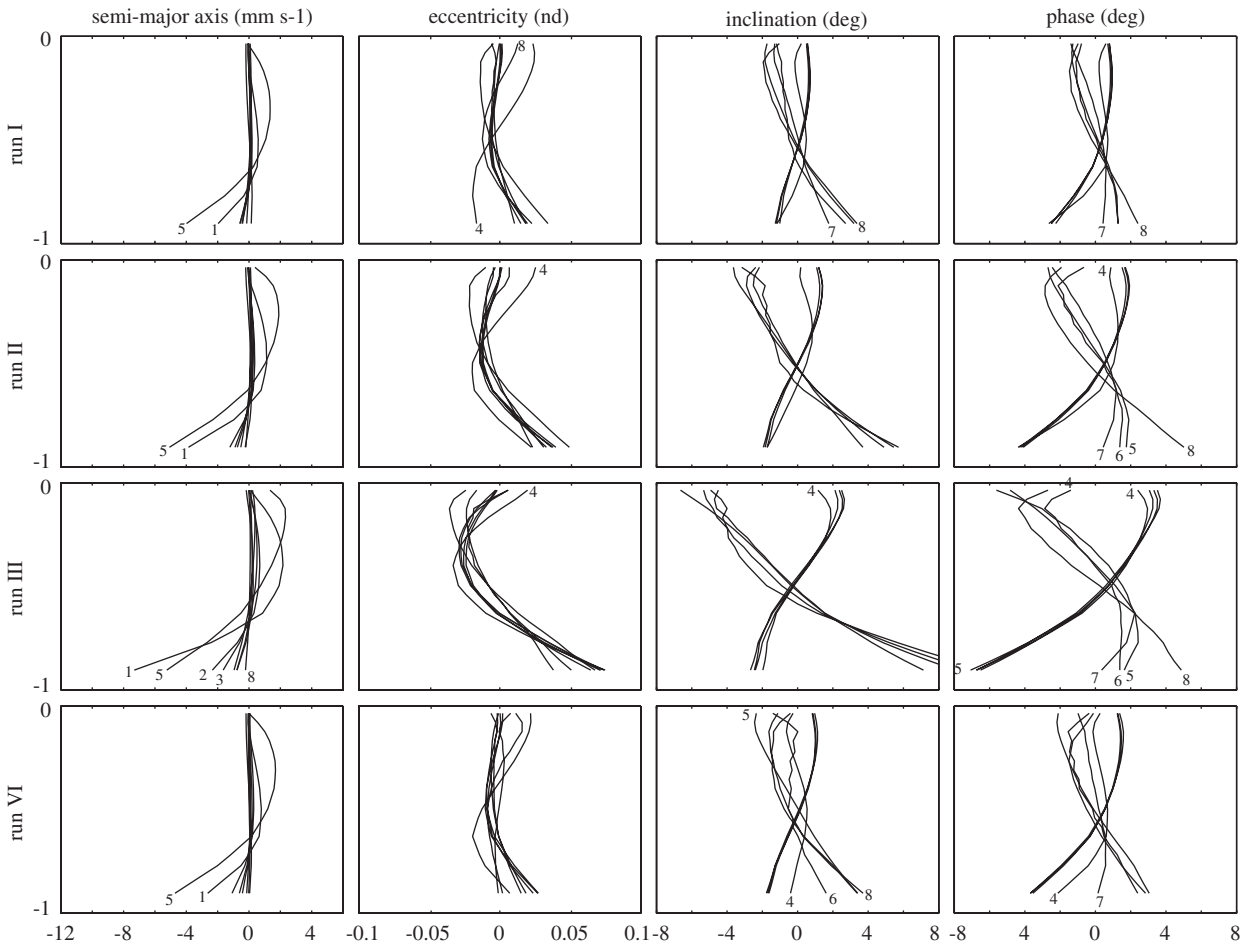

Fig. 11. Vertical structure of the tidal ellipses parameters at the shelf station I.4 (shown in Fig. 7a). The bold lines correspond to the semi-diurnal harmonics M_2, S_2, N_2 and K_2 (with numbers 1–4), and the thin lines correspond to the diurnal components K_1, O_1, P_1 and Q_1 (with numbers 5–8). Rows correspond to runs I–IV (see Table 2).

lines correspond to the semi-diurnal harmonics M_2, S_2, N_2 and K_2 (with numbers 1–4), and the thin lines correspond to the diurnal components K_1, O_1, P_1 and Q_1 (with numbers 5–8). Like in previous figures, here again the mean value of the parameters was removed. In the rows one to three, the linear bottom friction was used with the drag coefficient increasing twice from run I to run II and from run II to run III (run II used a typical parameterisation and was the one analysed until here). In the last run it was used a quadratic bottom friction parameterisation, as described previously.

We realise that runs I to III are qualitatively very similar, but the variation of the ellipse parameters with depth increases with the bottom drag coefficient. This leads to a higher distinction between the behaviours of the diurnal and semi-diurnal components, mainly in terms of the ellipse inclination and phase angle. The run IV is in general more similar with run two, without quantitatively signicative differences. This result was expected since run two and four correspond to typical parameterisations used in ocean modelling, in spite of the first (run II) be linear and the other (run VI) quadratic. One final simulation without bottom friction was also done. As result, the tidal currents become barotropic in the entire region. Also no distinction between semi-diurnal and diurnal vertical variation of parameters was possible.

4. Discussion and conclusions

A description of tidal dynamics of the Western Iberian Peninsula was obtained by means of

numerical modelling, putting emphasis on the study of the vertical structure of tidal ellipses for the homogeneous case. Stratification effects are beyond the scope of this study. It is well known that the stratification has influence on tidal ellipses (Souza and Simpson, 1996, Simpson 1997, Xing and Davies, 1997, 1998). However, in this study it has not been considered to avoid studying the many different situations concerning the stratification along the year for this region. Thus, the obtained results describe the winter situation in which the shelf is nearly homogeneous (Oliveira et al., 2004). As the main results for tidal heights amplitude and phase are similar to the previous literature (Fanjul et al., 1997) and compares well with the observations, no large efforts in validation for these results has been done. However, comparison of tidal ellipses for two points in the inner and middle shelf with currentmeters registers shows a good agreement. The tidal currents in the domain are dominated the semi-diurnal M_2 component and are amplified in the shelf. The diurnal components suffer a greater amplification, specially K_1 over the Lisbon Promontory. The analysis of vertical parameters of tidal ellipses allows a clear separation between semi-diurnal and diurnal components, and between the almost barotropic open sea circulation and the depth dependent, due to bottom friction, shelf currents.

Acknowledgements

Financial support for this study, a component of the project ProRecruit (POCTI/1999/BSE/36663), was supplied by Fundação para a Ciência e Tecnlogia (FCT). Martinho Marta Almeida was supported by a FCT PhD grant (SFRH/BD/5439/2001). Financial support was allocated by FCT under the Support Community Framework III, Operational Programme Science, Technology and Innovation. The authors thank to IPIMAR-INIAP for the data used in Fig. 8.

References

Davies, A.M., Kwong, S.C.M., Flather, R.A., 1997. Formulation of a variable-function three-dimensional model, with applications to the M_2 and M_4 tide on the North-West European Continental Shelf. Continental Shelf Research 17, 165–204.

de Mesquita, A.R., 2003. On the harmonic constants of tides and tidal currents of the South-eastern Brazilian shelf. Continental Shelf Research 23, 1227–1237.

Egbert, G., Bennett, A., Foreman, M., 1994. TOPEX/POSEIDON tides estimated using a global inverse model. Journal of Geophysical Research 99, 24821–24852.

Egbert, G.D., Erofeeva, S.Y., 2002. Efficient inverse modeling of barotropic ocean tides. Journal of Atmospheric and Oceanic Technology 19, 183–204.

Fanjul, E.A., Gómez, B.P., Sánchez-Arévalo, I.R., 1997. A description of tides in the Eastern North Atlantic. Progress in Oceanography 40, 217–244.

Fortunato, A., Pinto, L., Oliveira, A., Ferreira, J.S., 2002. Tidally generated shelf waves o the western Iberian coast. Continental Shelf Research 22, 1935–1959.

Haidvogel, D.B., Arango, H., Hedstrom, K., Beckman, A., Malanotte-Rizzoli, P., 2000. Model evaluation experiments in the North Atlantic Basin: simulations in nonlinear terrain following coordinates. Dynamics of Atmospheres and Oceans 32, 239–281.

Large, W.G., McWilliams, J.C., Dony, .C., 1994. Oceanic vertical mixing: A review and a model with nonlocal boundary layer parameterization. Reviews of Geophysics 32, 363–404.

New, A.L., da Silva, J., 2002. Remote-sensing evidence for the local generation of internal soliton packets in the central Bay of Biscay. Deep Sea Research Part I 49, 915–934.

Oliveira, P.B., Peliz, Á., Dubert, J., Rosa, T.L., Santos, A.M.P., 2004. Winter geostrophic currents and eddies in the western Iberia coastal transition zone. Deep Sea Research I 51, 367–381.

Pawlowicz, R., Beardsley, B., Lentz, S., 2002. Classic tidal harmonic analysis including error estimates in MATLAB using T TIDE. Computers and Geosciences 28, 929–937.

Pereira, A.F., Beckmann, A., Helmmer, H.H., 2002. Tidal mixing in the southern Weddell Sea: results from a tree-dimensional model. Journal of Physical Oceanography 32, 2151–2170.

Prandle, D., 1982. The vertical structure of tidal currents and other oscillatory flows. Continental Shelf Research 1, 191–207.

Prandle, D., 1997a. The influence of bed friction and vertical eddy viscosity on tidal propagation. Continental Shelf Research 17, 1367–1374.

Prandle, D., 1997b. Tidal currents in shelf seas—their nature and impacts. Progress in Oceanography 40, 245–261.

Pugh, D.T., 1987. Tides, Surges and Mean Sea Level. Wiley, New York.

Santos, A.M.P., Peliz, A., Dubert, J., Oliveira, P.B., Angélico, M.M., Ré, P., 2004. Impact of a winter upwelling event on the distribution and transport of sardine (*Sardina pilchardus*) eggs and larvae off western Iberia: a retention mechanism. Continental Shelf Research 24, 149–165.

Sauvaget, P., David, E., Soares, C.G., 2000. Modelling tidal currents on the coast of Portugal. Coastal Engineering 40, 393–409.

Simpson, J.H., 1997. Physical processes in ROFI regime. Journal of Marine Systems 12, 3–15.

Song, Y., Haidvogel, D., 1994. A semi-implicit ocean circulation model using a generalized topography-following coordinate system. Journal of Computational Physics 115, 228–244.

Souza, A.J., Simpson, J.H., 1996. The modification of tidal ellipses by stratification in the Rhine ROFI. Continental Shelf Research 16, 997–1007.

Vitorino, J., Oliveira, A., Jouanneau, J.M., Drago, T., 2002. Winter dynamics on the northern Portuguese shelf. Part 1: physical processes. Progress in Oceanography 52, 129–153.

Xing, J., Davies, A.M., 1997. Influence of stratification upon diurnal tidal currents in shelf edge regions. Journal of Physical Oceanography 29, 1803–1831.

Xing, J., Davies, A.M., 1998. A three-dimensional model of internal tides on the Malin-Hebrides shelf and shelf edge. Journal of Geophysical Research 103, 27821–27847.